

Article

An Effective Hybrid-Energy Framework for Grid Vulnerability Alleviation under Cyber-Stealthy Intrusions

Abdulaziz Almalqa^{1,*}, Saleh Albadran¹, Amer Alghadhban¹, Tao Jin² and Mohamed A. Mohamed^{3,*}

¹ Department of Electrical Engineering, Engineering College, University of Ha'il, Ha'il 55476, Saudi Arabia; s.abadran@uoh.edu.sa (S.A.); a.alghadhban@uoh.edu.sa (A.A.)

² Department of Electrical Engineering, Fuzhou University, Fuzhou 350116, China; jintly@fzu.edu.cn

³ Electrical Engineering Department, Faculty of Engineering, Minia University, Minia 61519, Egypt

* Correspondence: a.almalqa@uoh.edu.sa (A.A.); dr.mohamed.abdelaziz@mu.edu.eg (M.A.M.)

Abstract: In recent years, the occurrence of cascading failures and blackouts arising from cyber intrusions in the underlying configuration of power systems has increasingly highlighted the need for effective power management that is able to handle this issue properly. Moreover, the growing use of renewable energy resources demonstrates their irrefutable comparative usefulness in various areas of the grid, especially during cascading failures. This paper aims to first identify and eventually protect the vulnerable areas of these systems by developing a hybrid structure-based microgrid against malicious cyber-attacks. First, a well-set model of system vulnerability indices is presented to indicate the generation unit to which the lines or buses are directly related. Indeed, we want to understand what percentage of the grid equipment, such as the lines, buses, and generators, are vulnerable to the outage of lines or generators arising from cyber-attacks. This can help us make timely decisions to deal with the reduction of the vulnerability indices in the best way possible. The fact is that employing sundry renewable resources in efficient areas of the grid can remarkably improve system vulnerability mitigation effectiveness. In this regard, this paper proposes an outstanding hybrid-energy framework of AC/DC microgrids made up of photovoltaic units, wind turbine units, tidal turbine units, and hydrogen-based fuel cell resources, all of which are in grid-connect mode via the main grid, with the aim to reduce the percentage of the system that is vulnerable. To clearly demonstrate the proposed solution's effectiveness and ease of use in the framework, a cyber-attack of the false data injection (FDI) type is modeled and developed on the studied system to corrupt information (for instance, via settings on protective devices), leading to cascading failures or large-scale blackouts. Another key factor that can have a profound impact on the unerring vulnerability analysis concerns the uncertainty parameters that are modeled by the unscented transform (UT) in this study. From the results, it can be inferred that vulnerability percentage mitigation can be achieved by the proposed hybrid energy framework based on its effectiveness in the system against the modeled cyber-attacks.

Keywords: index terms-energy management; blackout; vulnerability; microgrid; energy framework; unscented transform; cyber-attack

MSC: 94-11



Citation: Almalqa, A.;

Albadran, S.; Alghadhban, A.;

Jin, T.; Mohamed, M.A. An Effective

Hybrid-Energy Framework for Grid

Vulnerability Alleviation under

Cyber-Stealthy Intrusions.

Mathematics **2022**, *10*, 2510.

<https://doi.org/10.3390/math10142510>

Academic Editor:

Juan Eloy Ruiz-Castro

Received: 22 June 2022

Accepted: 15 July 2022

Published: 19 July 2022

Publisher's Note: MDPI stays neutral with regard to jurisdictional claims in published maps and institutional affiliations.



Copyright: © 2022 by the authors. Licensee MDPI, Basel, Switzerland. This article is an open access article distributed under the terms and conditions of the Creative Commons Attribution (CC BY) license (<https://creativecommons.org/licenses/by/4.0/>).

1. Introduction

In recent decades, the AC/DC microgrid cloud has become the center of attention for most investigations that concern growing DC demands and the ease of use of renewable energy generations (REG). An AC/DC hybrid structure would be more controllable and more flexible in comparison with an independent structure due to the employment of varied electronic converters [1]. Along the same vein, the authors in [2] have proposed an energy scheduling of AC/DC resources. It is important to take into consideration how to dispatch energy among the different resources that were surveyed in [3] in the form of a decentralized structure. A game-theory-based solving method is investigated in [4], by which

coordinating the energy management of the hybrid network is no concern. Reference [5] has offered a decentralized-based operation approach that reaches a global optimal solution for hybrid energy configuration. This method takes into account a three-level problem separately consisting of the voltage source converter seating, DC microgrid, and AC microgrid. In [6], the objective functions of AC/DC microgrids are optimally satisfied based on an approach inspired by the multi-objective concept. The authors in [7] have aimed to minimize both the energy loss and total cost related to a hybrid microgrid with help of bi-level-based multi-objective management. Needless to say, a close look at the energy scheduling of microgrids reveals some undeniable concerns in their ignoring the uncertain effects of renewable energy generations. In light of this evidence, there is much that can be achieved to address the issue constructively. Reference [8] has moderately eliminated the above concern and presented Taguchi's orthogonal array-based absorbing approach, aiming to model uncertain parameters. Also, an energy management approach that takes into account the uncertainty framework of the AC/DC hybrid network is described in [9]. In this investigation, the authors have modeled not only the uncertainty effects, but the correlation structure among parameters as well. Briefly, structures that are made up of varied renewable energy units suffer correlated impacts that pertain to uncertain parameters like solar radiation, wind blow, and so on, which must be addressed. In the context of the correlation, the unscented transform (UT) method may be the best approach [9]. Ultimately, when hybrid microgrids are in a grid-connected mode via the smart main grid, the electrical grid could be more controllable and more flexible compared to the unforeseen faults and threats, such as cyber-attacks, that arise from the misuses of the "smartness" concept. In other words, as smart devices can increase accuracy and controllability, so do cyber out-lawed intrusions aim to wreck system performance. Not having a safe cyber platform can undoubtedly raise the risk of unauthorized access due to the usage of smart devices. One of the most perilous and important attacks in the context of the power systems described in [10] is the false data injection, or FDI, attack. Reference [11] indicates how FDI attacks could overshadow energy scheduling in the electrical grid. Authors in [12] have tried to provide an all-inclusive review of FDIA. Being efficient and effective, such attacks become evident if they are not detected by grid operators. On this basis, Ref. [13] carried out an FDIA and indicated that corrupting information related to monitoring devices would overshadow the optimal performance of the grid. A type of cyber-attack without the need for system data, named blind FDIA, was first introduced by [14]. Vulnerable areas of the grid risk becoming the target goals of a hacker in order to cause the most sabotage. In the technical sense, the vulnerability indices definitively illustrate which areas in the system are weakest against unforeseen faults. Accordingly, the vulnerable points of the system that lead to cascading faults and blackouts must first be identified. Many investigations have been conducted in the context of this issue. In the literature, researchers have indicated that cascading outages, and in turn, blackouts, are launched if the protective devices in the system have not been guaranteed against hidden faults. A study in [15] reported that protective devices are involved in 75% of the main disruptions of a system. In recent years, the widespread blackouts in the United States made an impression on a vast number of customers. To avoid future repetition of such cases, grid operation must be examined from a vulnerability analysis perspective [16]. Such an analysis can help in the development of the weak and susceptible points in a system, protecting against all contingencies to establish an invulnerable grid [17]. In this regard, some studies [18–20] have tried to provide accurate yet varied models of vulnerability indices. Having looked at these approaches, it can be inferred that assessing vulnerability is based on (1) dynamic vulnerability evaluation and (2) steady-state vulnerability evaluation [21]. So, to make a non-vulnerable grid, the sensitive and critical points of the grid must be protected against probable faults, which may or may not be purposefully exploited by cyber attackers. To this end, this paper suggests a collaborative energy framework for the electrical grid to improve vulnerability indices, employing the hyperactive available capacity of the various renewable energy resources. Indeed, we provide a hybrid microgrid made up of AC resources such as wind turbines and tidal

turbines, combined with DC energy resources including the PV system and fuel cell unit to deal with the defined issue. Such a hybrid system can facilitate timely decisions to inject power into the grid to alleviate vulnerability percentages, resulting in the hindrance of blackouts. For the main differences that differentiate this paper from others, see Table 1. Authors in [22] have presented a seconder control system using the AC microgrid to reduce vulnerability in a grid. Also, Ref. [23] has examined the effects of grid vulnerability from the perspective of cyber-attacks. The authors proved the extent to which vulnerability indices can be improved by shifting from a DC microgrid. Papers [8,10] present AC/DC microgrids in a consideration of the effects of uncertainty on energy management.

Table 1. Categorization of the different approaches.

	AC Microgrid	DC Microgrid	Vulnerability	Uncertainty	Cyber Attack
[8]	✓	✓		✓	
[10]	✓	✓			✓
[22]	✓		✓		
[23]		✓	✓		✓
Proposed model	✓	✓	✓	✓	✓

Broadly speaking, this paper aims to make the following contributions:

- Identification and mitigation of the vulnerable areas of the electrical grid by developing a microgrid structure based on a hybrid-energy framework that employs AC/DC renewable resources.
- Modeling and development of a cyber-attack of FDI type and adapted with a vulnerability analysis that aims to launch cascading faults and blackouts in a power system.
- Analysis of the proposed hybrid-energy framework in the uncertainty model using the unscented transform (UT) method to get the unerring vulnerability analysis.

The rest of the paper is structured as follows: Section 2 represents the vulnerability analysis formulation. Section 3 shows how the proposed hybrid framework is formulated. Section 4 shows how the uncertainty modeling is examined. The relevant consequences are indicated in Section 5, and in conclusion, the outcomes of the paper are described.

2. The Model of the Proposed Vulnerability Analysis

Growing loads and grid structure complexity are convincing reasons to believe that there is a rising chance of emergent cascading faults and blackouts [24]. These issues may affect social welfare due to lack of access to a grid that may serve industrial and residential demands [25]. To overcome the problem, the sensitive and overriding areas within the electrical grid, known as the vulnerability points, must be identified and evaluated [26]. When cascading faults are launched that are entirely due to structural associations within the grid, a vulnerability analysis can help identify the generating unit of lines and buses with the corresponding percentage. Keeping this in mind, this paper seeks to describe a structural association matrix-based vulnerability model as adapted to a power system. Following this, a cyber-attack model of the FDI type is developed that is capable of launching a malicious attack aimed at causing blackouts. For better realization, assume a studied electrical grid including k lines, n buses, and u generation units. When a fault or several faults for any reason within the grid concurrently occur, the lines and generation units have a high risk of being offline compared to the other equipment. Likewise, the outage effects of the lines and generation units on the other section of the grid, which are not directly related to the fault, must also be examined, as described in the following section.

2.1. The Bus Vulnerability Indices

Having looked at the above description, the vulnerability value of all buses for disconnecting line k is computed as shown below [15]:

$$N_n^k = \left(\frac{1 - dV_{min,n}}{1 - dV_{n,k}} \right)^2 \times \left(\frac{(1 - dV_{normal,n}) - (1 - dV_{n,k})}{(1 - dV_{normal,n}) - (1 - dV_{min,n})} \right)^2 \tag{1}$$

$$VIN_n^k = \begin{cases} 1 \rightarrow N_n^k > N_n^{basic} \\ 0 \rightarrow N_n^k < N_n^{basic} \end{cases} \tag{2}$$

Equation (1) indicates the vulnerability value of a bus n based on the current bus voltage (or voltage deviation) when the line k is offline. It is worth noting here that the outage of a line may affect the voltage value of buses owing to alterations in the flowing current in lines. Hence, getting the voltage variation, rather than the normal value, from the grid buses can be a significant criterion for assessment of the vulnerability of buses. If this value surpasses the basic amount, the bus index (VIN) is calculated as 1 and is otherwise 0. It is worth noting here that taking into account the threshold value (basic value) for the vulnerability indices limits the problem, bringing an optimal and safe solution and providing a timely decision for a decision-making center during contingencies. Hence, it can be inferred from (1) that the vulnerability value (N_b^k) will be equal to 0 if the bus voltage undergoes no change under the normal and current statuses.

2.2. The Line Vulnerability Indices

In the same way, the outage effects of line k on the other lines of the grid can be an outstanding criterion for assessing the vulnerability value of the grid lines, as shown in Equations (3) and (4).

$$K_l^k = \left(\frac{PL_l^k}{PL_l^{max}} \right)^2 \times \left(\frac{PL_l^k - PL_{normal,l}^k}{PL_l^{max} - PL_l^k} \right)^2 \tag{3}$$

$$VIK_l^k = \begin{cases} 1 \rightarrow K_l^k > K_l^{basic} \\ 0 \rightarrow K_l^k < K_l^{basic} \end{cases} \tag{4}$$

When a blemish is launched, the flowing power of the lines undergoes a marked alteration due to the looping circuit of the grid. Hence, the vulnerability value of lines can be calculated based on the flowing power during the fault occurrence (line k outage). In this regard, Equation (3) brings the vulnerability assessment of line l under the line k outage. Finally, if the line l index is equal to 1, in accordance with Equation (4), then the line k outage can directly affect line l and vice versa.

2.3. The Generation Unit Vulnerability Indices

Due to tenacious protective planning, generation units are more easily damaged than other equipment in contingency events. Hence, this section is dedicated to modeling the relationship between the generation unit u and the line k outage. It is important to note that the load demands are optimally satisfied by the active/reactive powers of the generation units by means of the grid lines. Therefore, getting lines out of reach causes non-optimal alteration in the power generated by these units. Keeping this in mind, relations (5) and (6) show the vulnerability value of the generation unit u when the contingency related to the line k outage occurs. Looking at (5), once a fault in the grid occurs, if the generator power increases up to a normal level, then the generator’s performance is vulnerable to the outage of line k . Therefore, evaluating the vulnerability of generators is dependent on the active power generation, with an emphasis on their max/min limitations of power. This description is expandable to the reactive power generation of generators. Meanwhile, the vulnerability indices of the active/reactive powers are calculated in accordance with (7) and (8) [15].

$$U_u^k = \left(\frac{P_u^{grid,k} - P_{normal,u}^k}{P_u^{max} - P_u^{min}} \right)^2 \times \max \left[\left(\frac{P_u^{min}}{P_u^{grid,k}} \right)^2, \left(\frac{P_u^{grid,k}}{P_u^{max}} \right)^2 \right] \tag{5}$$

$$UQ_u^k = \left(\frac{Q_u^{grid,k} - Q_{normal,u}^k}{Q_u^{max} - Q_u^{min}} \right)^2 \times \max \left[\left(\frac{Q_u^{min}}{Q_u^{grid,k}} \right)^2, \left(\frac{Q_u^{grid,k}}{Q_u^{max}} \right)^2 \right] \tag{6}$$

$$VIU_l^k = \begin{cases} 1 \rightarrow U_u^k > U_u^{basic} \\ 0 \rightarrow U_u^k < U_u^{basic} \end{cases} \tag{7}$$

$$VIUQ_l^k = \begin{cases} 1 \rightarrow UQ_u^k > UQ_u^{basic} \\ 0 \rightarrow UQ_u^k < UQ_u^{basic} \end{cases} \tag{8}$$

Following these calculations, the vulnerability indices related to the buses, lines, and the generation units under the line k outage are saved and inserted into the matrix \vec{KO} .

$$\vec{KO} = \begin{matrix} \xleftrightarrow{k:1,2,\dots,L} \\ \begin{bmatrix} \vec{VIN} \\ \vec{VIK} \\ \vec{VIUQ}, \vec{VIU} \end{bmatrix} \end{matrix} \tag{9}$$

Also, to obtain the vulnerability assessment of the grid in relation to the undesirable outage of a generation unit u , the computing process must be reiterated by means of the relations (3) to (9). Hence, the indices matrix pertaining to the outage of a generation unit u is obtained by (10) [15].

$$\vec{UO} = \begin{matrix} \xleftrightarrow{u:1,2,\dots,G} \\ \begin{bmatrix} \vec{VIN} \\ \vec{VIK} \\ \vec{VIUQ}, \vec{VIU} \end{bmatrix} \end{matrix} \tag{10}$$

To achieve the disturbance ratio of the contingencies over the buses, lines, and generation units, i.e., the generation unit and line outage indices (NLO, NGO), the matrixes \vec{KO}, \vec{UO} must be denormalized based on the element number of the grid (R), as shown in (11) and (12).

$$NLO = \frac{\vec{KO}}{R} \tag{11}$$

$$NGO = \frac{\vec{UO}}{R} \tag{12}$$

Finally, the objective function of the vulnerability analysis is provided by Equation (13) considering NLO, NGO :

$$VUL = \sum_R NLO + NGO \tag{13}$$

3. The Cyber-Attack Model of the FDI Type

The wide usage of smart devices within the grid offers a number of targets for the menacing intent of a cyber-attacker. Indeed, cyber-intrusions into the controlling structure of an electrical grid or its critical areas, such as its vulnerability points may bring about irreparable injuries, along with declining social welfare. Hence, this section aims to model a perilous attack type named FDIA. Generally, an attack model can be categorized into one of three classes: (1) attack tree, (2) attack networks, (3) attack graphs. The first class aims to scan the structure of network nodes to carry out an intrusion based on its acyclic directed graph. As they model stealthy intrusions, the attack models in the attack network class are known as the trusty model. The third class describes attacks for which an attack graph is introduced as their backing point. Having looked at these definitions, it can be deduced

that the FDI attack belongs to the second class, as it aims to manifest a destructive impact on system performance. In this attack, it is important to assume that the hacker has a high chance of gaining access to the information of the studied system. On this basis, the FDI attack, by means of injecting incorrect information into the system as defined by (14), is launched, with an arbitrary performance targeted defined as in (15). Attack assessment is checked by constraint (16). In other words, assume that a system will reach an acceptable solution F given the injection of accurately measured data w_t to the system model $f()$ at time t , as shown in (14). Similarly, an illusory solution F_λ will be brought based on (15) by analyzing the system model $f()$ using false data $w_{bad,t}$ which is generated by a hacker based on the function (17) at the time J . Comparison of the system outcomes (F, F_λ) indicates whether or not the system's performance is affected more by the sudden change than by the errors in the measured devices that were introduced by the attacker (see Equation (16)).

$$F = f(w_t) \tag{14}$$

$$F_\lambda = f(w_{bad,t}) \tag{15}$$

$$F_\lambda - f(w_{bad,t}) = F - f(w_t) \tag{16}$$

Introduction of the false information is carried out by adding sufficient noise (z_t) to the measuring data or the device setting before monitoring. Formally, injecting the false data at time J is described as:

$$w_{bad,t} = \begin{cases} w_t + z_t & \text{if } t \geq J \\ w_t & \text{otherwise} \end{cases} \tag{17}$$

4. The Proposed Hybrid Energy Framework of Microgrid

In recent research, microgrids performance has shown that they can help grid energy operation become more controllable and more flexible in critical conditions, namely cascading faults and blackouts [27]. Keeping this in mind, this paper presents an outstanding hybrid energy framework of AC/DC microgrids that aim to reduce grid vulnerability toward targeting from cyber-attackers. The hybrid microgrid is introduced as an efficient solution that employs all AC and DC energy sources in an environmentally friendly energy framework [28]. To aid visualization of the proposed hybrid microgrid, Figure 1 depicts the developed structure, including the photovoltaic units, wind turbine units, tidal turbine units, and hydrogen-based fuel cell resources. In this section, the mathematical framework of the proposed microgrid is presented.

4.1. AC Microgrid

In the technical sense, microgrids that take into account the energy resource type employed are classified into three classes: DC microgrid, AC microgrid, and integrated energy resource-based microgrid. This section describes an AC microgrid composed of a tidal turbine system and wind turbine (WT) units. The alternative structure of these renewable sources is a persuasive reason for their inclusion into the AC microgrid class [8]. That said, such resources are also being applied in DC microgrid contexts with the use of varied electronic converters. Having looked at the WT structure, it can be inferred that wind speed and WT output power are in a straightforward relationship, such that altering wind speeds due to weather results in disquieting fluctuations in output power. The same holds true for tidal turbines in terms of current speed and output power. All in all, the mathematical objective function followed by resources and the relevant constraints are defined by (18)–(20).

$$C^m = \min \sum_{t \in \Omega^T} W_t^{WT} P W_t + T I_t^{tidal} P T_t \tag{18}$$

$$P W_t = \frac{1}{2} \rho S l (V e_t)^3 \quad \forall t \in \Omega^T \tag{19}$$

$$P_{T_t} = \begin{cases} 0 & 0 \leq C_t \leq C_{rated} \\ 0.5H_p\rho_1S_1C_t^3 & C_{cutin} \leq C_t \leq C_{rated} \\ P_{T_{rated}} & C_{rated} \leq C_t \end{cases} \quad \forall t \in \Omega^T \quad (20)$$

The objective function (18) incorporates both WT units and the tidal system. As noted previously, renewable resource owners have tendencies toward decreasing the energy cost with regards to the energy price, which is provided on an hourly basis by the energy market. Likewise, we write the objective function based on the minimization problem. Equation (19) indicates how to fulfill the output power of WT given knowledge of the wind speed. As can be seen, the function establishes a relationship with the cube of the wind speed, which has a geometric influence on the output power. The power generated by the tidal system is obtained with an emphasis on the varied ranges of the current speed in accordance with (20). It is clear that the output power is detachable in its reliance on current speed changes [29].

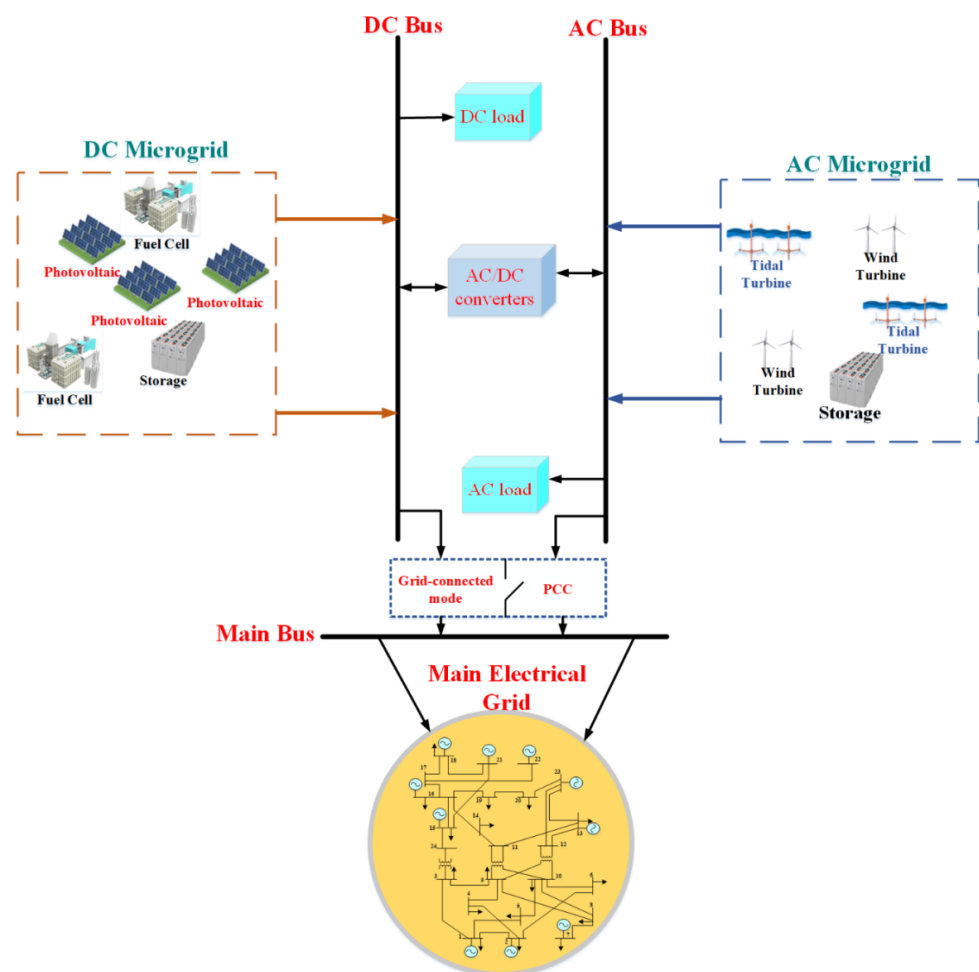


Figure 1. The proposed hybrid energy framework.

4.2. DC Microgrid

The DC microgrid structure defined in this paper includes DC renewable energy units such as the hydrogen generation-based fuel cell system and photovoltaic units equipped with a storage system. It is worth noting that, in order to predict the remaining useful life of the storage system, a useful method has been proposed in [30]. Such a microgrid aims to satisfy the DC demands and even AC demands with the use of electronic converters. What follows is a description of the one-to-one performance of DC generation units. The proton exchange membrane fuel cell (PEMFC) is the best among the various types of fuel cell units

defined in the literature. The fuel required by PEMFC in order to generate electrical power is molecular hydrogen, H₂. The hydrogen value needed to fulfill the output power is calculated by (23) and (24), by which the generated hydrogen is determined based on the total output power of the fuel cell units and the limitations of the hydrogen tanker. On the other hand, the function of the storage unit is to support demands under critical conditions. This means that dynamic fluctuations in demand can be covered by the storage units at every hour. Hence, the total output power results in the summation of the storage and fuel cell powers as indicated in (21). Also, the limits of the output capacity can be defined by (22) [31].

$$P_t^{Cell} = P_t^{FCcell} + P_t^{Cell_B} \quad \forall t \in \Omega^T \tag{21}$$

$$P_{cell}^{min} \leq P_t^{FCcell} + P_t^{Cell_B} \leq P_{Cell}^{max} \quad \forall t \in \Omega^T \tag{22}$$

$$0 \leq Hg_2^t \leq Hg_2^{max} \quad \forall t \in \Omega^T \tag{23}$$

$$Hg_2^t = (P_t^{FCcell} + P_t^{Cell_B}) \times \frac{3.6 \frac{MJ}{kWh}}{119.96 \frac{MJ}{Kg}} \quad \forall t \in \Omega^T \tag{24}$$

PV units are the other DC resources employed within the DC microgrid. The relationship between the output power and the solar radiation in PV is a well-established fundamental interaction based on (25): as solar radiation increases, so does the power generation in the PV unit. It can be clearly indicated that the generated power calculation may obtain an irregular outcome if PV loss is ignored in the computing process. Also, cooperation between the storage and PV units on supply for common demands can guarantee output power and neutralize fluctuations arising from solar radiation uncertainty. The constraints related to the storage unit are defined in accordance with (26)–(29). Looking at (26), the storage unit’s output power is determined by considering the charging/discharging power and also the power consumed in the fuel cell unit. The energy level of the battery is also checked every hour based on Equation (27). The storage unit is allowed to perform with an emphasis on its charging/discharging power limitations and the permissible energy level, as shown in (28) and (29). Finally, the objective function of the proposed DC microgrid is followed by (30) [29].

$$PV_t^{PV} = \frac{SA \times C_t^{PV}}{g} \times (1 - PV^{loss}) \quad \forall t \in \Omega^T \tag{25}$$

$$P_t^{bat} = P_t^{bat_ch} - P_t^{bat_dis} + P_t^{Cell_B} \quad \forall t \in \Omega^T \tag{26}$$

$$Eg_t^{Bat} = Eg_{t-1}^{Bat} + (P_t^{bat_ch} - P_t^{bat_dis})\eta^{Bat} \quad \forall t \in \Omega^T \tag{27}$$

$$P^{min} \leq P_t^{bat_ch}, P_t^{bat_dis} \leq P^{max} \quad \forall t \in \Omega^T \tag{28}$$

$$E^{min} \leq Eg_{n,t}^{Bat} \leq E^{max} \quad \forall t \in \Omega^T, \forall b \in \Omega^b \tag{29}$$

$$C^{total_dc} = \min \sum_{t \in \Omega^T} C_t^{pv} PV_t^{pv} + C_t^{Cell} P_t^{Cell} + (P_t^{bat_ch} - P_t^{bat_dis}) \times C_t^b \tag{30}$$

$$PW_t + PT_t + PV_t^{PV} + P_t^{Cell} + P_t^{bat_ch} - P_t^{bat_dis} = P_t^{dc_load} + P_t^{ac_load} \quad \forall t \in \Omega^T \tag{31}$$

$$C^{total} = C^{total_dc} + C^{total_ac} \tag{32}$$

A cooperative energy framework between the AC/DC microgrids can help satisfy AC/DC demands in a reliable and optimal way. To this end, Equation (31) expresses a power balance among the generation units and loads within the hybrid energy structure. In this relation, the right-hand term includes the output powers related to all AC/DC generation units aiming to supply the AC/DC demands, which are defined in the opposing term. In sum, the total cost of the hybrid microgrid is defined by Equation (32).

4.3. The Mathematical Formulation of the Main Grid

As previously discussed, we assume that the hybrid microgrid is in a grid-connected mode with the main grid and aims to improve grid vulnerability. Hence, the fundamental formulation of the main grid needs to be provided. It must first be mentioned that the electrical grid consists of fossil-fuel-based generator units, lines, and loads. Grid energy management with the goal of satisfying loads should fulfill an optimized energy schedule such that the total cost, including the active/reactive power cost of generators and start-up/shut-down cost, is minimized (see Equation (33)). Maintenance of technical constraints such as power balance and power generation limitations is another task that demands the adherence of the operator. Hence, Equations (34) and (45) introduce the technical limitations of the grid. Establishing balanced power between the generation units and the load demands of the lines is necessary to bring power sustainability to the grid in an optimal way. Therefore, we here define the power balance via (38) and (39). The generation units are subject to constraints (34) and (35). Note that ramping constraints for the generators must always be considered to prevent probable technical damage due to load fluctuations. Hence, the ramping power related to the generators is limited by (36) and (37), where the relationship between the generators and loads is established by the networking structure of lines in the grid. Therefore, modeling the flowing power of lines can help us understand the grid's behavior in pursuit of an optimal solution. Keeping this in mind, we here model the flowing power of lines (see Equations (40) and (41)) based on the bus voltage and angle difference, which are constrained by (42) and (43), which must be sustained within the allowed limits as indicated in (44) and (45). All in all, having looked at the vulnerability analysis, it becomes clear that the indices have a sensibility toward the grid variables, including the flowing power, the power generation, and voltages of buses, in comparison to their normal values. Indeed, the vulnerability percentage of this grid will decrease if the variables regarding operation of the grid are conserved at the standard level. To this end, the proposed hybrid microgrids can be useful in the relaxation of the grid variables using the power transaction described in Equations (38) and (39), which leads to a remarkable diminution in the generators' power, along with a lowering of the flowing power and voltage value as described in Equations (40) and (41). This results in the reduction of the vulnerability percentage while taking into account Equations (1), (3), (5), and (6). In sum, the proposed model comprises the objective function (32), (33), and (13) and the relevant constraints defined by equations (19) to (31) and (34) to (45). In addition to these constraints, to establish the awareness-arising of the grid vulnerability analysis, Equations (1)–(12) are considered as the problem constraints while operating the grid.

$$C^{grid} = \min \sum_t \sum_u [C(P_{u,t}^{grid}) + U_{u,t}^{grid} + D_{u,t}^{grid}] \tag{33}$$

$$P_u^{min} u_{u,t} \leq P_{u,t}^{grid} \leq P_u^{max} u_{u,t} \quad \forall t \in \Omega^T \tag{34}$$

$$Q_u^{min} u_{u,t} \leq Q_{u,t}^{grid} \leq Q_u^{max} u_{u,t} \quad \forall t \in \Omega^T \tag{35}$$

$$P_{u,t}^{grid} - P_{u,t-1}^{grid} \leq R_{grid}^+ u_{u,t-1} \quad \forall t \in \Omega^T \tag{36}$$

$$P_{u,t-1}^{grid} - P_{u,t}^{grid} \leq R_{grid}^+ u_{u,t} \quad \forall t \in \Omega^T \tag{37}$$

$$\sum_{\forall u(n)} (P_{u,t}^{grid}) - \sum_{\forall k(n,m)} (PL_{l,t}) + P_t^{Microgrid} = Pl_{b,t} \quad \forall t \in \Omega^T, \forall n \in \Omega^n \tag{38}$$

$$\sum_{\forall u(n)} Q_{u,t}^{grid} + \sum_{\forall k(n,m)} (QL_{l,t}) = Ql_{b,t} \quad \forall t \in \Omega^T, \forall n \in \Omega^n \tag{39}$$

$$PL_l = (dV_n - dV_m)gb_l - bg_l\delta_l, \quad \forall m \in \Omega^m, \forall n \in \Omega^n, \forall l \in \Omega^l \tag{40}$$

$$QL_l = -(1 + 2dV_n)bg_{l0} - (dV_n - dV_m)bg_l - gb_l\delta_l, \quad \forall m \in \Omega^m, \forall n \in \Omega^n, \forall l \in \Omega^l \tag{41}$$

$$\delta_l^{min} \leq \delta_{l,t} \leq \delta_l^{max} \quad \forall t \in \Omega^T, \forall l \in \Omega^l \tag{42}$$

$$dV_{min,n} \leq dV_{n,t} \leq dV_{max,n} \quad \forall t \in \Omega^T, \forall n \in \Omega^n \tag{43}$$

$$- PL_l^{max} \leq PL_{l,t} \leq PL_l^{max} \quad \forall t \in \Omega^T, \forall l \in \Omega^l \tag{44}$$

$$- QL_l^{max} \leq QL_{l,t} \leq QL_l^{max} \quad \forall t \in \Omega^T, \forall l \in \Omega^l \tag{45}$$

5. The Uncertainty Model

Due to the presence of renewable resources, a close look at the uncertainty model can enhance hybrid microgrid operation. Hence, this section is dedicated to presenting an efficient approach to accurately modeling the behavior of uncertain parameters within the microgrid and the electrical grid. Regarding renewable resources, we here consider the sunlight, wind speed, tidal current variations, and load demands that are defined in both the electrical grid and the microgrid. We show that the UT method has the ability to model these uncertain parameters, including demand, the output power of PV, WT, and tidal units, and the fuel cell power, as well as their correlation. In the literature, the UT method has been introduced as a useful tool for mapping uncertain parameters based on a correlated transformation [32]. The advantages of this method are evident in its ease of coding and low computing time, as well as its high ability to address uncertainty and provide a correlational environment. Indeed, the UT method makes the approximation of a probability distribution function (pdf) easier than a nonlinear function [32]. To make the awareness-arising of this method, we propose modeling the uncertainty of the problem as $U = \hat{f}(R)$, in which U is the problem outcome, $\hat{f}()$ is the uncertainty function, and (R) is the input. For p uncertain parameters in the problem, the length of input vector R is p with regard to the mean value ∂ and covariance S_{aa} with standard deviation ω . It is worth here noting that the elements of the matrix S_{aa} are made up of the variance and covariance of the various uncertain parameters. Hence, the UT approach can produce an acceptable solution that considers p uncertain variables $2p + 1$ times. All in all, the steps of this model are described in (46)–(51).

Step 1: the covariance matrix related to $2p + 1$ points is calculated as follows:

$$R^0 = \partial \tag{46}$$

$$P^k = m + \left(\sqrt{\frac{p}{1 - W^0} S_{aa}} \right)_a \quad a = 1, 2, \dots, p \tag{47}$$

$$P^{k+p} = m - \left(\sqrt{\frac{p}{1 - W^0} S_{aa}} \right)_a \quad a = 1, 2, \dots, p \tag{48}$$

Step 2: the weight of all points is computed via (47) and (48):

$$W^k = \frac{1 - W^0}{2p} \quad a = 1, 2, \dots, 2p \tag{49}$$

Step 3: in the last step, the output value is obtained based on the points and weight calculated in steps 1 and 2.

In this step, the output vector F^k must first be obtained based on $f()$ and points P^k along with their weights, which were calculated in the previous step. Then, vector \bar{F} can be computed with regards to Equation (50) for the summation of all points. Following that, the UT technique uses Equation (51) to reach the mean ∂ and covariance matrix P_{FF} of the output U .

$$\bar{F} = \sum_{a=0}^{2p} W^k F^k \tag{50}$$

$$P_{FF} = \sum_{a=1}^{2p} W^k (F^k - \bar{F}) (F^k - \bar{F})^T \tag{51}$$

6. Simulation Results

Cooperation on common tasks between the microgrid and the main electrical grid with the goal of mitigating vulnerability may be an appropriate solution. To this end, this paper proposes a hybrid energy framework for AC/DC microgrids that are in the grid-connected mode. To do so, an attack model of FDI type was launched with the aim of demolishing the vulnerable areas within the electrical grid. In this studied system, the hybrid microgrid includes some number of AC/DC renewable energy units, including PV, fuel cell, WT, and tidal systems, with an emphasis on maintaining the relevant technical limitations. Information related to renewable energy resources is described in detail in [33,34]. In addition, the electrical grid structure based on the IEEE 24-bus test system was defined in accordance with [35,36].

6.1. Relieving Grid Vulnerability Based on the Proposed Strategy

As previously mentioned, this paper aims to follow an efficient hybrid microgrid-based energy framework with help from an unerring vulnerability model to identify and mitigate vulnerable areas in a grid, which can result in cascading faults due to malevolent cyber intrusions. That said, the primary goal is to describe the performance of microgrids and how they exchange energy with the main electrical grid in the context of an environmentally friendly hybrid energy framework. Consequently, the applicability of the proposed framework for improving grid vulnerability indices as much as possible was also examined. Hence, Figure 2 indicates the generated power of the DC sources, including PV and fuel-cell units, in terms of scheduling for power injection into the hybrid bus through the corresponding electronic converters. It is clear that the PV unit received more demand than the others, owing to more solar radiation at those times. The low energy price of the fuel cell unit at $t = 14$ is mainly due to more power being injected by the fuel cell compared to the PV unit. Further, Figure 3 shows the generated power related to the AC units in the hybrid energy framework. As can be seen, the WT and tidal turbine units generate the needed power at some hours, with an emphasis on energy price and technical limitations such as wind speed and current speed. Having looked at Figures 2 and 3, it can be inferred that the renewable units have no power generation at $t = 1-3$ and $t = 21-23$. This means that the microgrid loads are satisfied by the grid-connected link at these hours. To justify this elucidation, Figure 4 depicts the power transaction between the proposed hybrid microgrid and the main electrical grid. The star points in this figure show the accurate amount of power exchanging between the grids. It is necessary to note that the positive power exchange indicates energy being trading from the grid to the hybrid microgrid and vice versa.

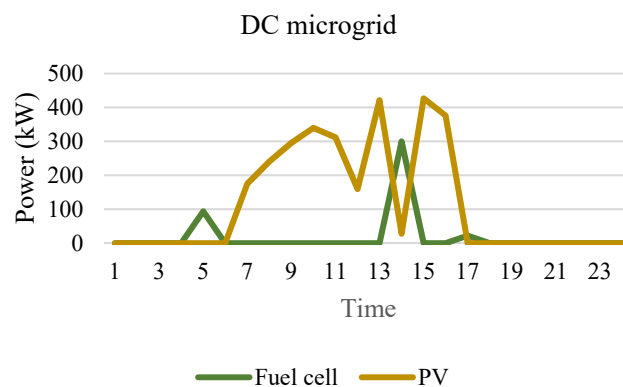


Figure 2. The generated powers of DC units including PV and fuel cell units.

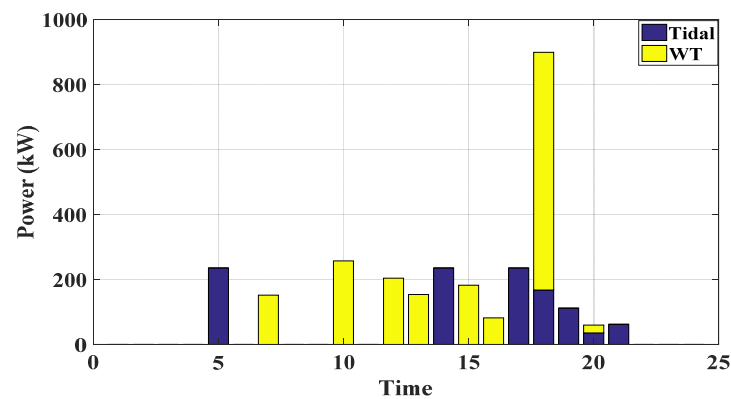


Figure 3. The generated powers of AC units including wind and tidal turbines.

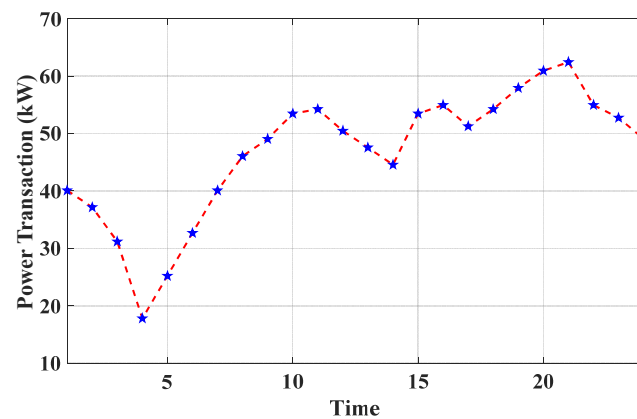


Figure 4. The power exchanged between the grid and the hybrid microgrid.

The vulnerability assessment may be the most significant analysis of the electrical grid due to the irreparable destruction that arises from cascading faults or blackouts. Indeed, when a fault occurs for any reason, some vulnerable areas that emerge due to the looping structure of the grid (especially transmission) are always overshadowed by the fault effects that finally lead to blackouts. Hence, identifying and reducing the grid’s vulnerable points is a must. To this end, this paper provides a vulnerability assessment model and proposes a hybrid energy framework that aims to improve the vulnerability indices of the grid. To do so, we considered a proficient hacker that obtains access to system information and deploys an FDI attack by injecting erroneous data, with the goal of launching a cascading fault. Hence, we implemented the proposed hybrid energy framework and analyzed grid performance with the help of the vulnerability model. To further test the proposed framework’s effectiveness, we compared the grid’s vulnerability indices based on two strategies: (*strategy1*), the hybrid energy framework, and (*strategy2*), ignoring the proposed microgrid. Figures 5–11 indicate the relevant consequences under three different scenarios: (1) outage of line 2 in the 24-bus system, (2) outage of the generation unit 4 in the 24-bus system, (3) outage of line 3 in the 24-bus system.

At this point, there was a need to determine whether or not the proposed strategy could influence grid operation towards reducing the effects of contingent events on the performance of the lines and generators to prevent blackouts in the grid. This was accomplished by implementing the vulnerability analysis on the energy management of the grid. The relevant results from this analysis are indicated in Figures 5–8. As can be seen, the results are for two strategies: (1) strategy 1 and (2) strategy 2, previously defined. Hence, Figure 5 shows the vulnerability percentage of generators for strategy 2. As can be seen, the vulnerability percentages for the generators are classified by three different ranges, including four generators in the range of 9 to 11, another four generators in the range of 11 to

13, and finally, two generators in the range of 13 to 15. It can be inferred from these results that the vulnerability percentages were obtained based on strategy 1 with max/min ranges of 9 and 15, respectively. Meanwhile, the vulnerability percentages for generators based on strategy 2 took a range of 4 to 12, as shown in Figure 6. This means that the proposed hybrid framework could enable a remarkable reduction of almost 65% in the vulnerability of generators. In this context, Figures 7 and 8 illustrate the vulnerability of lines for both strategies. As can be seen, the vulnerability percentages of all lines based on the proposed hybrid structure decreased in the realm of 25% compared to strategy 2, which also testifies to the proposed model’s effectiveness. In addition, looking at the vulnerability model, it can be inferred that the generation units and the lines have the greatest risk of outage due to the setting of the protective devices. Hence, analyzing the NGOI and NLOI indices in the vulnerability model is significant. By doing so, the comparative results show that the hybrid energy framework leads to a marked slump in the NLOI indices compared to strategy 1 (see Figure 9). Similar to the line outage, comparing the NGOI indices under different scenarios proves the proposed framework’s effectiveness in reducing the generation unit vulnerability of the electrical grid, as indicated in Figure 10. Also, Figure 11 shows the comparative results related to the total cost of the grid for both strategies, which reveal a tendency toward reduction in grid energy cost under the proposed hybrid energy framework.

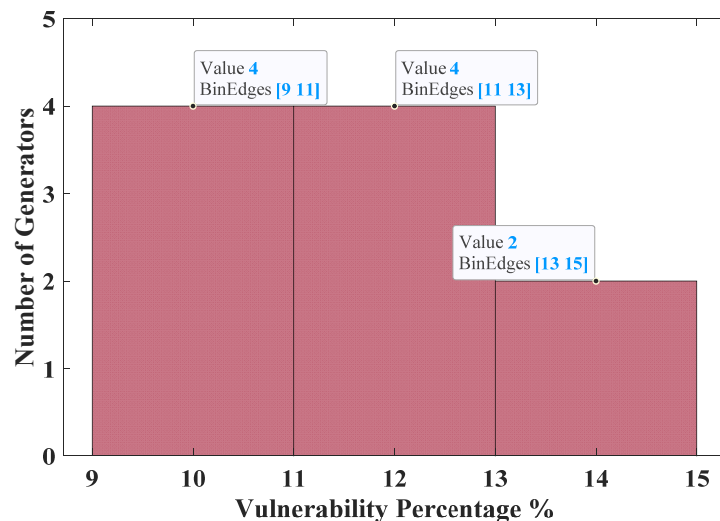


Figure 5. The vulnerability analysis of the generators for strategy 2.

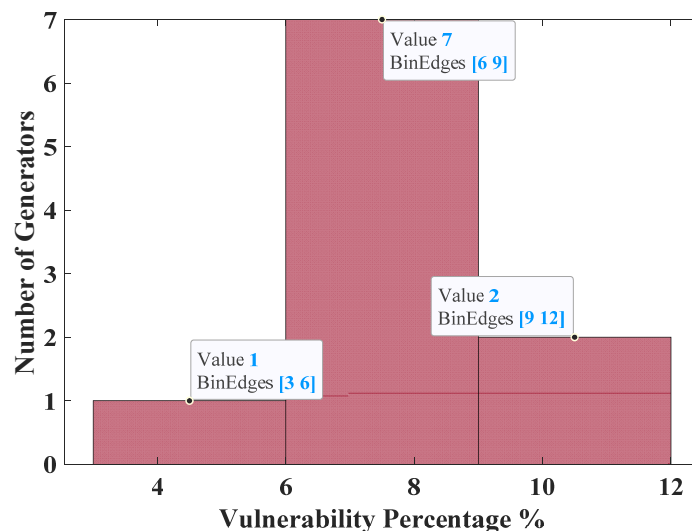


Figure 6. The vulnerability analysis of the generators for strategy 1.

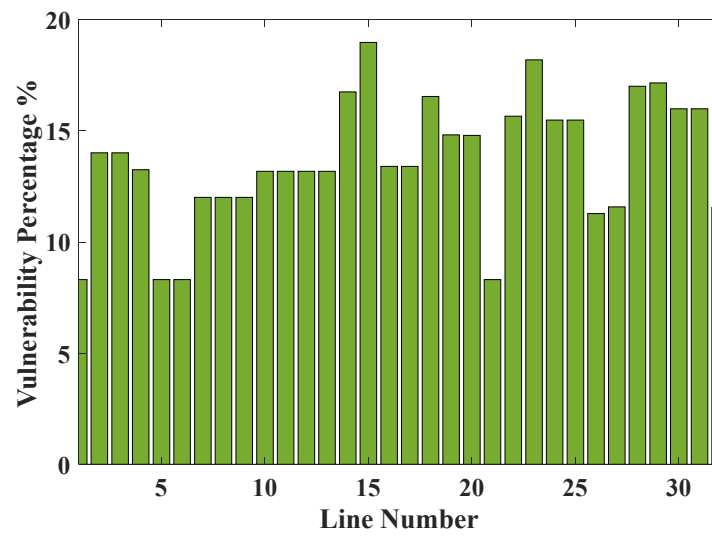


Figure 7. Illustration of the vulnerability analysis of the lines for strategy 2.

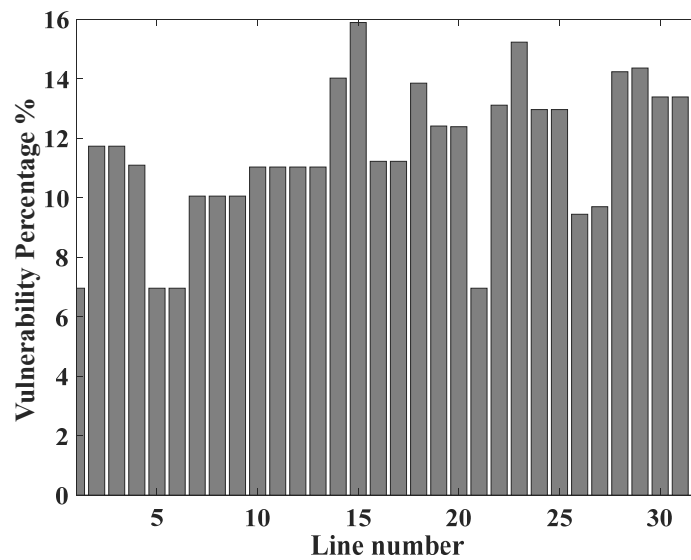


Figure 8. Illustration of the vulnerability analysis of the lines for strategy 1.

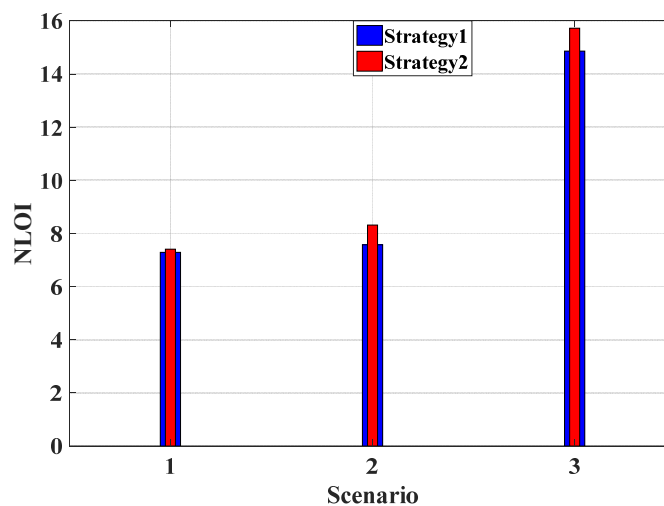


Figure 9. The comparative result of the NLOI indices.

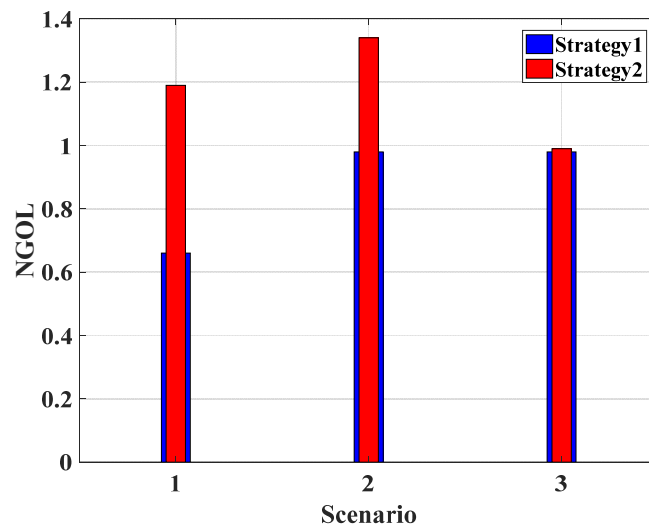


Figure 10. The comparative result of the NGOI indices.

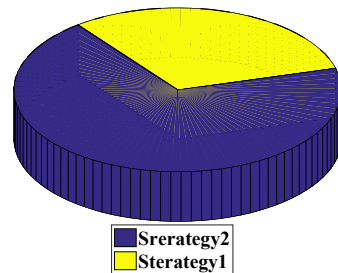


Figure 11. The total cost of the grid for strategy 1 and strategy 2.

6.2. The Performance of the Uncertainty Model

To properly evaluate the proposed hybrid framework, the grid performance must be examined using the uncertainty model due to its effectiveness in finding an accurate solution. The uncertain parameters of the hybrid microgrid include the current speed of the tidal unit, solar radiation, and wind speed, as well as the load demands. It is worth mentioning that the parameters that have remarkable fluctuations (at the SD level) can affect energy scheduling if they are not precisely forecasted via an uncertainty model. In addition, correlation among these uncertain parameters is another issue that needs to be addressed. As already seen, the UT approach would bring accurate forecasting and correlation to the uncertain parameters. Note that information on input data such as those for wind speed, tidal current, and solar radiation can be found in detail in [31]. To model the uncertainty of these parameters, there is a need for their time-continuous mean and variance values, all of which are derived in detail from [31]. It is worth noting here that this study considers a normal distribution function for solar radiation and load demands, while the Weibull distribution function is used for modeling wind speed and tidal current. Hence, we implemented the UT method, considering the wind speed, tidal current, and solar radiation, and provided the output vectors, including the output powers of WT, tidal turbine, and PV, in Figures 12–15. We have indicated the outcomes of the uncertainty model for the output power of WT, the output power of the tidal turbine, and the output power of PV based on the normal and uncertainty scenarios in Figures 12–14. As can be seen in Figure 12, the wind speed based on the uncertainty model had remarkable changes in the output power at some hours compared to the normal scenario. These changes in the output powers of WT resulted from the uncertainty in the wind speed. Similarly, such alterations can also be seen in the output power of the tidal turbine in a comparison of both scenarios, as shown in Figure 13. Looking at Figure 14, the solar radiation uncertainty model reveals

the alteration of the output power of PV systems for most hours. The comparative results of the total cost under the normal and stochastic statuses are indicated in Figure 15. It can be seen that uncertainty-based energy scheduling could create a high fluctuation of almost 3.36% in the total cost, which means that consideration of grid analysis, such as its vulnerability under the uncertainty framework, is a must.

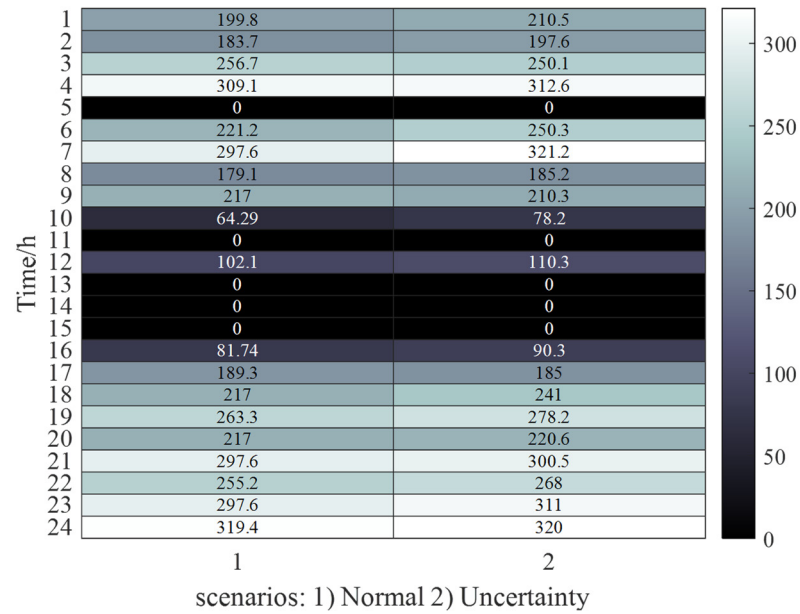


Figure 12. The output power of wind turbines for both scenarios.

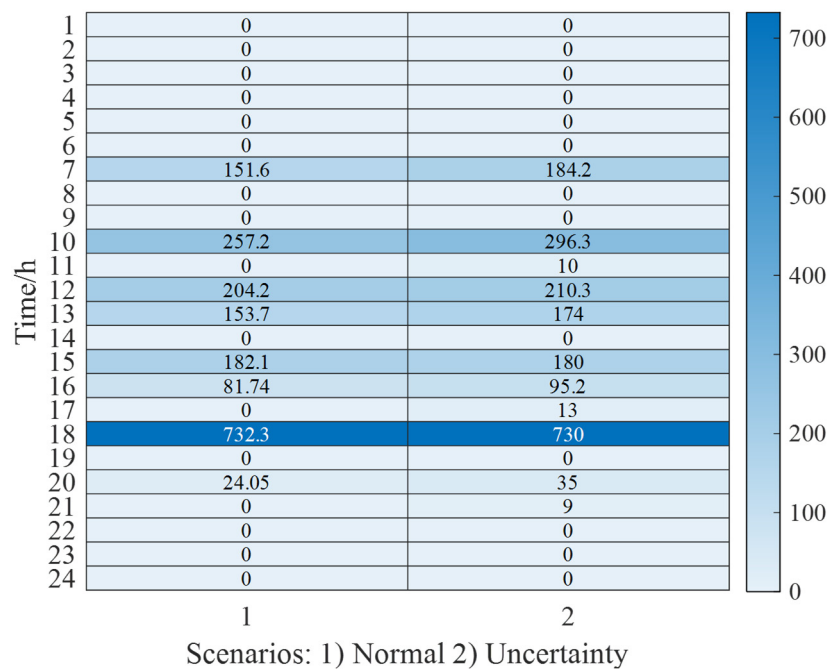


Figure 13. The output power of the tidal turbine for both scenarios.

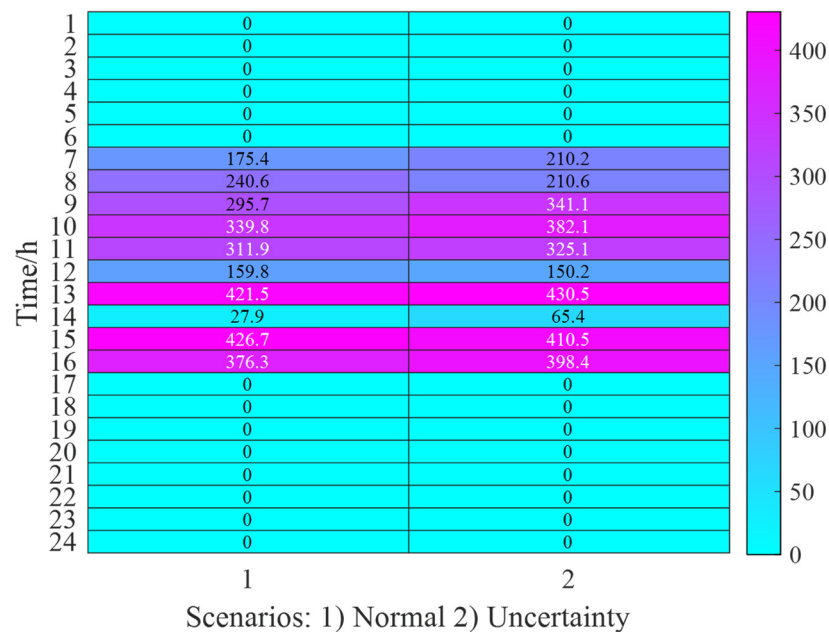


Figure 14. The output power of the PV system for both scenarios.

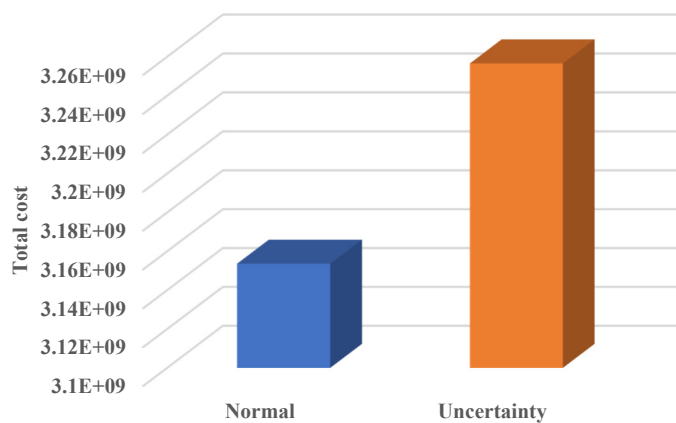


Figure 15. Total cost under uncertainty framework.

7. Conclusions

This paper is dedicated to finding an appropriate solution by which grid vulnerability could decline in order to prevent the cascading faults arising from cyber stealthy intrusions. To this end, a hybrid energy framework that is compatible with the vulnerability analysis model was suggested. Also, a cyber-attack of the FDI type was modeled to simulate corruption of the setting of protective devices to precipitate the launch of cascading faults into the grid. We described a hybrid microgrid in the grid-connected mode that aims to inject/receive the needed power to/from the grid to sustain it or reduce its vulnerability indices as much as possible. Following this, an analysis of grid vulnerability was conducted and its relevant consequences were described, as provided in the Results section. The comparative outcomes indicate that the proposed hybrid framework could realize a remarkable reduction of almost 10% in the vulnerability indices for the varied scenarios of generation unit and line outages. Moreover, our results show that the vulnerability analysis in the grid would be more accurate and more flexible if energy scheduling could be precisely forecasted based on an uncertainty model. For future work, we suggest that the proposed hybrid structure be extended into different research areas, such as resilience analysis of the electrical grid, in order to return and stabilize grid operation in the context of cyber-attacks that aim to cause blackouts in the grid.

Author Contributions: Conceptualization, A.A. (Abdulaziz Almalaq), S.A., A.A. (Amer Alghadhban), T.J. and M.A.M.; methodology, A.A. (Abdulaziz Almalaq), T.J. and M.A.M.; software, A.A. (Abdulaziz Almalaq), S.A., A.A. (Amer Alghadhban) and M.A.M.; validation, S.A., A.A. (Amer Alghadhban), T.J. and M.A.M.; formal analysis, A.A. (Abdulaziz Almalaq) and M.A.M.; investigation, A.A. (Amer Alghadhban), S.A., A.A. (Amer Alghadhban), T.J. and M.A.M.; data curation, A.A. (Abdulaziz Almalaq), S.A., A.A. (Amer Alghadhban), T.J. and M.A.M.; writing—original draft preparation, A.A. (Abdulaziz Almalaq), S.A., A.A. (Amer Alghadhban), T.J. and M.A.M.; writing—review and editing, A.A. (Abdulaziz Almalaq), S.A., A.A. (Amer Alghadhban), T.J. and M.A.M.; visualization, A.A. (Abdulaziz Almalaq), S.A., A.A. (Amer Alghadhban), T.J. and M.A.M.; supervision, M.A.M.; project administration, A.A. (Abdulaziz Almalaq), S.A., A.A. (Amer Alghadhban), T.J. and M.A.M.; funding acquisition, A.A. (Abdulaziz Almalaq), S.A., A.A. (Amer Alghadhban). All authors have read and agreed to the published version of the manuscript.

Funding: This research has been funded by Scientific Research Deanship at University of Ha'il—Saudi Arabia through project number RG-21079.

Institutional Review Board Statement: Not applicable.

Informed Consent Statement: Not applicable.

Data Availability Statement: Not applicable.

Conflicts of Interest: The authors declare no conflict of interest.

Nomenclature

Sets/Indices

l/Ω^l	Set/index for feeder
u/Ω^u	Set/index for power unit
t/Ω^T	Set/index for hour
$n, m/\Omega^{n,m}$	Set/index of bus bar

Limitations

SA	Solar energy
PV^{loss}	PV losses
C_t	Tidal current speed
C_{cutin}, C_{rated}	Tidal cut-in speed and rated speed
g	Direct irradiation
ρ, ρ_1	Seawater and wind densities
S	Brushed area of the turbine blades
l	Rotor blade area
bg_l, gb_l, bg_{l0}	Technical characteristics of line
$U_{u,t}^{grid}, D_{u,t}^{grid}$	Unit start-up, shut down
$H_{g,t}^t, P_t^{min,Cell}, P_t^{max,Cell}$	Hydrogen mass, min/max limitations of fuel cell power.
C_t^{PV}	PV Capacity
$w_{bad,t}, w_t$	Manipulated and normal data
Ve_t	Current speed of tidal
PT_{rated}	Rated generation of tidal
E_t^{min}, E_t^{max}	High/low limits for storage system
$P_t^{dc_load}, P_t^{ac_load}$	Microgrid demands
P_u^{min}, P_u^{max}	Active power limitations
PL_t^{min}, PL_t^{max}	Line active power limitations
QL_t^{min}, QL_t^{max}	Line reactive power limitations
Q_u^{min}, Q_u^{max}	Reactive power limitations
R_{grid}^+, R_{grid}^-	Up/down Limits of reserve
$dV_{min,n}, dV_{max,n}$	Limits of voltage
$\delta_t^{min}, \delta_t^{max}$	Limits of angle
$Pl_{b,t}$	Smart grid active demand in each bus
$Ql_{b,t}$	Smart grid reactive demand in each bus
C	Generation price of the generator.
$W_t^{WT}, TI_t^{tidal}, C_t^{pv}, C_t^{Cell}, C_t^b$	Bidding offer for WT, tidal, PV, fuel cell and battery
∂, ω	Mean and variance
W^0	weight of the mean value
S_{aa}	covariance matrix
R	vector of stochastic inputs

Variables

$P_i^{bat}, PW_i, PT_i, PV_i^{PV}, P_i^{Cell}, P_i^{FCCell}, P_i^{Cell_B}$	Generation amount of storage, WT, tidal, PV, and fuel cell units.
N_n^k	Line outage index of bus n
VIN_n^k	Bus index
K_l^k	Line outage index of line l
VIK_l^k	line index
U_u^k	unit outage active index of line l
VIU_u^k	unit index
UQ_u^k	unit outage reactive index of line l
$VIUQ_u^k$	unit index
VUL	The objective function
E_s^{bat}	Battery energy of PV
$Q_{u,t}^{grid}, QL_{l,t}$	Generator and feeder reactive power at time t.
$P_{u,t}^{grid}, PL_{l,t}$	Generator and line active power at time t.
$u_{u,t}$	Binary variables of the generator.
dV_n, δ_n	Bus voltage or angle.
C^{grid}, C^m	Operation cost functions of smart grid and microgrid.

References

- Esfahani, M.M.; Mohammed, O. Real-time distribution of en-route electric vehicles for optimal operation of unbalanced hybrid AC/DC microgrids. *eTransportation* **2019**, *1*, 100007. [\[CrossRef\]](#)
- Xu, Q.; Xiao, J.; Wang, P.; Wen, C. A decentralized control strategy for economic operation of autonomous AC, DC, and hybrid AC/DC microgrids. *IEEE Trans. Energy Convers.* **2017**, *32*, 1345–1355. [\[CrossRef\]](#)
- Azeem, O.; Ali, M.; Abbas, G.; Uzair, M.; Qahmash, A.; Algarni, A.; Hussain, M. A Comprehensive Review on Integration Challenges, Optimization Techniques and Control Strategies of Hybrid AC/DC Microgrid. *Appl. Sci.* **2021**, *11*, 6242. [\[CrossRef\]](#)
- Ekneligoda, N.C.; Weaver, W.W. Game-theoretic cold-start transient optimization in DC microgrids. *IEEE Trans. Ind. Electron.* **2014**, *61*, 6681–6690. [\[CrossRef\]](#)
- Golsorkhi, M.S.; Savaghebi, M. A Decentralized Control Strategy Based on V-I Droop for Enhancing Dynamics of Autonomous Hybrid AC/DC Microgrids. *IEEE Trans. Power Electron.* **2021**, *36*, 9430–9440. [\[CrossRef\]](#)
- Li, P.; Zheng, M. Multi-objective optimal operation of hybrid AC/DC microgrid considering source-network-load coordination. *J. Mod. Power Syst. Clean Energy* **2019**, *7*, 1229–1240. [\[CrossRef\]](#)
- Bhowmik, C.; Bhowmik, S.; Ray, A. Optimal green energy source selection: An eclectic decision. *Energy Environ.* **2020**, *31*, 842–859. [\[CrossRef\]](#)
- Hussain, A.; Bui, V.-H.; Kim, H.-M. Robust Optimal Operation of AC/DC Hybrid Microgrids Under Market Price Uncertainties. *IEEE Access* **2017**, *6*, 2654–2667. [\[CrossRef\]](#)
- Papari, B.; Edrington, C.S.; Bhattacharya, I.; Radman, G. Effective Energy Management of Hybrid AC–DC Microgrids With Storage Devices. *IEEE Trans. Smart Grid* **2017**, *10*, 193–203. [\[CrossRef\]](#)
- Alnowibet, K.; Annuk, A.; Dampage, U.; Mohamed, M.A. Effective Energy Management via False Data Detection Scheme for the Interconnected Smart Energy Hub–Microgrid System under Stochastic Framework. *Sustainability* **2021**, *13*, 11836. [\[CrossRef\]](#)
- Acosta, M.R.C.; Ahmed, S.; Garcia, C.E.; Koo, I. Extremely randomized trees-based scheme for stealthy cyber-attack detection in smart grid networks. *IEEE Access* **2020**, *8*, 19921–19933. [\[CrossRef\]](#)
- Rahman, A.; Mohsenian-Rad, H. False data injection attacks with incomplete information against smart power grids. In Proceedings of the 2012 IEEE Global Communications Conference (GLOBECOM), Anaheim, CA, USA, 3–7 December 2012; pp. 3153–3158.
- Dehghani, M.; Niknam, T.; Ghiasi, M.; Siano, P.; Alhelou, H.H.; Al-Hinai, A. Fourier Singular Values-Based False Data Injection Attack Detection in AC Smart-Grids. *Appl. Sci.* **2021**, *11*, 5706. [\[CrossRef\]](#)
- Julier, S.J. The scaled unscented transformation. In Proceedings of the 2002 American Control Conference (IEEE Cat. No. CH37301), Anchorage, AK, USA, 8–10 May 2002; Volume 6, pp. 4555–4559.
- Abedi, A.; Hesamzadeh, M.R.; Romero, F. An ACOPF-based bilevel optimization approach for vulnerability assessment of a power system. *Int. J. Electr. Power Energy Syst.* **2021**, *125*, 106455. [\[CrossRef\]](#)
- Chen, J.; Mohamed, M.A.; Dampage, U.; Rezaei, M.; Salmen, S.H.; Al Obaid, S.; Annuk, A. A Multi-Layer Security Scheme for Mitigating Smart Grid Vulnerability against Faults and Cyber-Attacks. *Appl. Sci.* **2021**, *11*, 9972. [\[CrossRef\]](#)
- Liu, Y.; Jin, T.; Mohamed, M.A.; Wang, Q. A Novel Three-Step Classification Approach Based on Time-Dependent Spectral Features for Complex Power Quality Disturbances. *IEEE Trans. Instrum. Meas.* **2021**, *70*, 1–14. [\[CrossRef\]](#)
- Zhang, Y.; Wang, L.; Xiang, Y.; Ten, C.-W. Inclusion of SCADA Cyber Vulnerability in Power System Reliability Assessment Considering Optimal Resources Allocation. *IEEE Trans. Power Syst.* **2016**, *31*, 4379–4394. [\[CrossRef\]](#)
- Doorman, G.; Uhlen, K.; Kjelle, G.; Huse, E. Vulnerability Analysis of the Nordic Power System. *IEEE Trans. Power Syst.* **2006**, *21*, 402–410. [\[CrossRef\]](#)
- Velloso, A.; Van Hentenryck, P. Combining Deep Learning and Optimization for Preventive Security-Constrained DC Optimal Power Flow. *IEEE Trans. Power Syst.* **2021**, *36*, 3618–3628. [\[CrossRef\]](#)
- Abedi, A.; Gaudard, L.; Romero, F. Power flow-based approaches to assess vulnerability, reliability, and contingency of the power systems: The benefits and limitations. *Reliab. Eng. Syst. Saf.* **2020**, *201*, 106961. [\[CrossRef\]](#)

22. Chen, J.; Alnowibet, K.; Annuk, A.; Mohamed, M.A. An effective distributed approach based machine learning for energy negotiation in networked microgrids. *Energy Strat. Rev.* **2021**, *38*, 100760. [[CrossRef](#)]
23. Abianeh, A.J.; Wan, Y.; Ferdowsi, F.; Mijatovic, N.; Dragicevic, T. Vulnerability Identification and Remediation of FDI Attacks in Islanded DC Microgrids Using Multiagent Reinforcement Learning. *IEEE Trans. Power Electron.* **2021**, *37*, 6359–6370. [[CrossRef](#)]
24. Mohamed, M.A.; Chen, T.; Su, W.; Jin, T. Proactive Resilience of Power Systems Against Natural Disasters: A Literature Review. *IEEE Access* **2019**, *7*, 163778–163795. [[CrossRef](#)]
25. Li, Y.; Wang, B.; Wang, H.; Ma, F.; Zhang, J.; Ma, H.; Zhang, Y.; Mohamed, M.A. Importance Assessment of Communication Equipment in Cyber-Physical Coupled Distribution Networks Based on Dynamic Node Failure Mechanism. *Front. Energy Res.* **2022**, *10*, 654. [[CrossRef](#)]
26. Ma, F.; Wang, B.; Zhou, J.; Jia, R.; Luo, P.; Wang, H.; Mohamed, M.A. An effective risk identification method for power fence operation based on neighborhood correlation network and vector calculation. *Energy Rep.* **2021**, *7*, 6995–7003. [[CrossRef](#)]
27. Ma, H.; Liu, Z.; Li, M.; Wang, B.; Si, Y.; Yang, Y.; Mohamed, M.A. A two-stage optimal scheduling method for active distribution networks considering uncertainty risk. *Energy Rep.* **2021**, *7*, 4633–4641. [[CrossRef](#)]
28. Mohamed, M.A.; Abdullah, H.M.; Al-Sumaiti, A.S.; El-Meligy, M.A.; Sharaf, M.; Soliman, A.T. Towards Energy Management Negotiation Between Distributed AC/DC Networks. *IEEE Access* **2020**, *8*, 215438–215456. [[CrossRef](#)]
29. Chabok, H.; Aghaei, J.; Sheikh, M.; Roustaei, M.; Zare, M.; Niknam, T.; Lehtonen, M.; Shafi-Khah, M.; Catalão, J.P. Transmission-constrained optimal allocation of price-maker wind-storage units in electricity markets. *Appl. Energy* **2022**, *310*, 118542. [[CrossRef](#)]
30. Liu, C.; Li, D.; Wang, L.; Li, L.; Wang, K. Strong robustness and high accuracy in predicting remaining useful life of supercapacitors. *APL Mater.* **2022**, *10*, 061106. [[CrossRef](#)]
31. Roustaei, M.; Niknam, T.; Salari, S.; Chabok, H.; Sheikh, M.; Kavousi-Fard, A.; Aghaei, J. A scenario-based approach for the design of Smart Energy and Water Hub. *Energy* **2020**, *195*, 116931. [[CrossRef](#)]
32. Zou, H.; Tao, J.; Elsayed, S.K.; Elattar, E.E.; Almalaq, A.; Mohamed, M.A. Stochastic multi-carrier energy management in the smart islands using reinforcement learning and unscented transform. *Int. J. Electr. Power Energy Syst.* **2021**, *130*, 106988. [[CrossRef](#)]
33. Mohamed, M.A. A relaxed consensus plus innovation based effective negotiation approach for energy cooperation between smart grid and microgrid. *Energy* **2022**, *252*, 123996. [[CrossRef](#)]
34. Roustaei, M.; Letafat, A.; Sheikh, M.; Chabok, A.; Sadoughi, R.; Ardeshiri, M. A cost-effective voltage security constrained congestion management approach for transmission system operation improvement. *Electr. Power Syst. Res.* **2022**, *203*, 107674. [[CrossRef](#)]
35. Tan, H.; Yan, W.; Ren, Z.; Wang, Q.; Mohamed, M.A. Distributionally robust operation for integrated rural energy systems with broiler houses. *Energy* **2022**, *254*, 124398. [[CrossRef](#)]
36. Tan, H.; Ren, Z.; Yan, W.; Wang, Q.; Mohamed, M.A. A Wind Power Accommodation Capability Assessment Method for Multi-Energy Microgrids. *IEEE Trans. Sustain. Energy* **2021**, *12*, 2482–2492. [[CrossRef](#)]